Operation Efficiency Optimization for Permanent Magnet Synchronous Motor Based on Improved Particle Swarm Optimization

Zheng Chen[1,2], Senior Member, IEEE, Wanchao Li[1], Xing Shu[1], Jiangwei Shen[1], Yuanjian Zhang[3], Member and Shiquan Shen[1]

[1]Faculty of Transportation Engineering, Kunming University of Science and Technology, Kunming, 650500, China.
[2]School of Engineering and Materials Science, Queen Mary University of London, London, E1 4NS, China.
[3]School of Mechanical and Aerospace Engineering, Queen's University of Belfast, BT9 5AG, Northern Ireland.

Corresponding author: Shiquan Shen (e-mail: 1158531507@qq.com).

ABSTRACT In this paper, an improved online particle swarm optimization (PSO) is proposed to optimize the traditional search controller for improving the operating efficiency of the permanent magnet synchronous motor (PMSM). This algorithm combines the advantages of the attraction and repulsion PSO and the distributed PSO that can help the search controller to find the optimal d-axis air gap current quickly and accurately under non-stationary operating conditions, thereby minimizing the air gap flux and then improving the motor efficiency. To verify the effectiveness and stability of this proposed algorithm, the operating efficiency of PMSM as using this proposed algorithm is compared with that of traditional search controller under non-stationary operating conditions. The results show that the proposed algorithm can improve the operating efficiency of PMSM by 6.03% on average under non-stationary operation conditions. This indicates that the search controller based on the improved PSO has a better adaptation to the variation of external operating conditions, and can improve the operation efficiency of PMSM under non-stationary condition.

INDEX TERMS permanent magnet synchronous motor, efficiency optimization, particle swarm optimization, golden section method.

I. INTRODUCTION

The consumption of fossil energy, environmental pollution, and greenhouse gas emissions caused by the burning of fossil energy are becoming increasingly serious [1]. Under such circumstances, compared with internal combustion engine vehicles, electric vehicles (EVs) due to its zero emissions, high efficiency, and stable operating systems have received more attention from various countries [2]. The motor as the main power output sources of EVs is the link between the energy storage system [3-5] and the wheels, can effectively increase the endurance mileage of EVs in a single charge as choosing the appropriate motor and improving the operating efficiency of the motor [6]. The permanent magnet synchronous motor (PMSM) due to its high efficiency, simple structure, reliable operation, and small size [7] is always selected as the power output machine for EVs [8]. Generally, there are two methods to improve the operating efficiency of PMSM. One method is to optimize the structure of electromagnetic to ensure that the PMSM has a high torque density and high reliability. In [9], a new type of electromagnetic structure for PMSM was developed to reduce the voltage distortion rate, and then to improve the efficiency of the PMSM. The other method is to develop a high-performance control strategy to reduce unnecessary losses during the PMSM operation. In general, the widely used control strategies include maximum torque per ampere (MTPA) control strategy [10], maximum torque per voltage (MTPV) control strategy [11], losses model controller (LMC) strategy [12], and search controller (SC) strategy [13].

In the MTPA control strategy, as the d-axis magnetic component of the stator current increases, the air gap magnetic field generated by the permanent magnetic component will be weakened, such field weakening control can effectively use the torque of PMSM, and increase the maximum torque output capacity, thereby improving the efficiency of PMSM. In [14], an infinite speed drives MTPA control was proposed to ensure that the automatic transition of different magnetic field regions can be realized before the magnetic flux is weakened. This method can effectively reduce the stator copper loss, therefore improving the PMSM efficiency. In [15], a new relationship

between torque, current amplitude, and current angle during optimal operation is established to calculate the current excitations in the MTPA control strategy, this method can accurately estimate the stator current, thereby reducing the copper loss error caused by calculation. However, the iron loss generated during the operation of PMSM is ignored in the MTPA control strategy that limits the further increase of motor efficiency [16]. In the MTPV control strategy, the iron loss generated during the operation of motor is also ignored, therefore its maximum efficiency is also limited.

In the LMC and SC control strategies, both the iron loss and the copper loss are considered that can maximize the efficiency of PMSM over the entire operating range. The LMC method needs to establish the PMSM equivalent circuit model firstly, and then use the equivalent circuit principle to derive an objective mathematical function related to the stator current. Since this function is a convex function, the convex optimization principle can be used to obtain the best stator current. In [17], a new iron loss calculation model was proposed for LMC strategy to reduce the computational burden. However, the algorithm performance is significantly affected by the PMSM parameters and surrounding environment. When the PMSM is running under non-stationary conditions, the accuracy of this algorithm will be greatly reduced.

The SC strategy applied in control circuit searches the appropriate d-axis current in a fixed range to achieve the field weakening effect, thereby improving the efficiency of the motor [18]. This method is independent of the motor parameters, therefore it is globally effective, robust, and has a high accuracy. In [19], a new algorithm was proposed to reduce iron loss by optimizing the traditional SC through combining fuzzy logic controller (FLC) and golden section method (GSM-SC). However, the traditional SC strategy is based on the static decoupling characteristic of the vector control algorithm, and as the optimization algorithm is implemented, the change in magnetic flux will destroy this characteristic and cause the fluctuation in the output torque [20]. In [21], in order to improve the operation efficiency of PMSM, traditional GSM-SC is used to obtain the optimal d-axis current by controlling the d-axis current based on the analysis of the PMSM loss model. But compared with LMC that can directly calculate and set the optimal magnetic flux according to the working conditions of PMSM, the GSM-SC requires the speed of PMSM to be constant as calculating the flux linkage under different torques, and sequentially adjust the optimization direction of the magnetic flux according to the size of the flux linkage. Thus, the calculation efficiency of GSM-SC is relatively slow [22].

The LMC and SC strategies are hard to be applied in the industrial controller directly due to the undesirable torque interference caused by the oscillation of air gap [23]. To meet the requirements of actual industrial production and overcome the shortcomings of these algorithms, some scholars fuse particle swarm optimization (PSO) into the SC to ensure that

the controller has the advantages of simplicity, easy implementation, fast convergence, and few adjustable parameters.

The improved SC based on the PSO has a simple structure, and its optimization goal is to maximize the operation efficiency directly at a given torque, thereby the PMSM efficiency is reasonably close to optimal value. In [24], an improved SC based on genetic algorithm (GA) and PSO is proposed, which can obtain satisfactory results for energy saving control, and greatly improves the search speed on the basis of the traditional SC. In [25], PSO was proposed to optimize the SC to obtain the optimized d-axis current, thereby minimizing the air gap flux and reducing the torque interference caused by the oscillation of air gap. These applications have proved the practicality of improved SC based on the PSO.

Although the PSO can improve the operating efficiency of PMSM, there are two problems for this algorithm, one is the convergence of this algorithm always leading to a local optimal value [25]. The other is the fitness value of each particle always changing in the dynamic environment. The particle always finds the optimal fitness value at a certain position in the last iteration that results in the fitness value may not be optimal in the next iteration [26]. Therefore, in the actual operation of EVs, the basic PSO is hard to find the optimal value [27].

To solve these two problems, an improved PSO (AR-DPSO) that combines the advantage of the attraction and repulsion PSO (ARPSO) and the distributed PSO (DPSO) is proposed to improve the searching ability of particle swarms to find the optimal value accurately and quickly under non-stationary operation conditions. This improved PSO can help particles to detect the change of motor speed, and make a self-adjustment for the change of speed under non-stationary conditions, thereby finding the optimal d-axis air gap current accurately and quickly, and then improving the operating efficiency of PMSM.

The main contributions of this study can be summarized as follows: 1) An AR-DPSO algorithm is proposed to establish the online SC control strategy to improve the operating efficiency of PMSM in non-stationary conditions through optimizing the d-axis air gap current; 2) The proposed AR-DPSO algorithm can improve the operating efficiency of the PMSM by 6.03% on average under non-stationary operation conditions as compared with the traditional search controller.

The rest of this paper is structured as follows: In Section II, the equivalent circuit model and loss formula for PMSM are introduced. Section III puts forward the AR-DPSO and the improved GSM-SC. Section IV carries out the simulation verification and compares the final experimental results for different control algorithms. Section V gives the concluding comments.

II. EQUIVALENT MODEL AND LOSS ANALYSIS OF PMSM

A. EQUIVALENT CIRCUIT MODELS

The equivalent circuit models for PMSM in the rotating-coordinate system are shown in Fig. 1 (a) and (b) respectively [28].
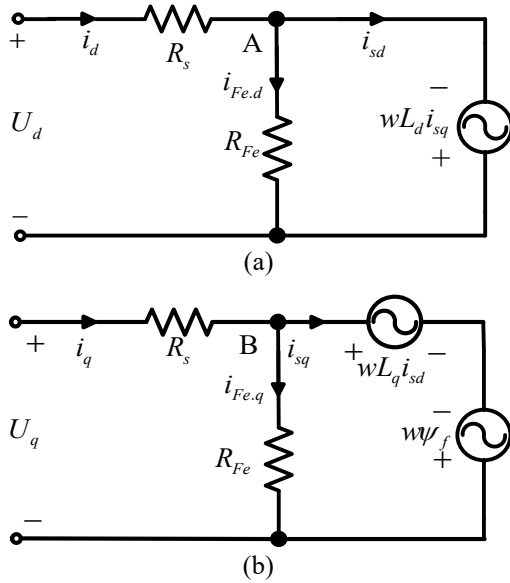

(a)

(b)

FIGURE 1. The equivalent circuit models for PMSM in the rotating-coordinate system. (a) d-axis. (b) q-axis.

In Fig. 1, U_d and U_q are the stator voltage components of the d-q axis respectively, i_d and i_q represent the stator current components of the d-q axis respectively, R_s denotes the stator winding resistance, i_{sd} and i_{sq} are the d-q axis air gap current components respectively, w denotes the PMSM speed, ψ_f is the permanent magnet flux linkage, n_p denotes the number of poles, R_{Fe} is the iron loss equivalent resistance, L_d and L_q represent d-q axis inductance components respectively, $i_{Fe.d}$ and $i_{Fe.q}$ are the d-q axis components of stator current based on iron loss respectively.

According to the equivalent circuit models, the stator flux linkage equation in the rotating-coordinate system is:

$$\begin{cases} \psi_d = L_d i_{sd} + \psi_f \\ \psi_q = L_q i_{sq} \\ \psi_s = \sqrt{\psi_d^2 + \psi_q^2} = \sqrt{(L_d i_{sd} + \psi_f)^2 + (L_d i_{sq})^2} \end{cases} \quad (1)$$

where ψ_s is the stator flux linkage, ψ_d and ψ_q represent the stator flux components of the d-q axis respectively. The electromagnetic torque of the PMSM in the rotating-coordinate system is:

$$T_e = \frac{3}{2} n_p (\psi_d i_{sq} - \psi_q i_{sd}) = \frac{3}{2} n_p [(L_d - L_q) i_{sd} i_{sq} + \psi_f i_{sq}] \quad (2)$$

where T_e is the electromagnetic torque. The node current equation of the PMSM equivalent circuit can be obtained from Fig. 1 as:

$$\begin{cases} i_d = i_{sd} + i_{Fe \cdot d} \\ i_q = i_{sq} + i_{Fe \cdot q} \end{cases} \quad (3)$$

The expression of the d-q axis component of the stator current based on iron loss can be obtained as:

$$\begin{cases} i_{Fe \cdot d} = -\dfrac{w L_q i_{sq}}{R_{Fe}} \\ i_{Fe \cdot q} = \dfrac{w(L_d i_{sd} + \psi_f)}{R_{Fe}} \end{cases} \quad (4)$$

The loop voltage equation of the PMSM equivalent circuit can be obtained from Fig. 1:

$$\begin{cases} u_d = R_s i_d - w L_q i_{sq} \\ u_q = R_s i_q + \omega L_q i_{sd} + w \psi_f \end{cases} \quad (5)$$

From (4) to (8), we can get:

$$i_{Fe \cdot d} = \frac{w L_q}{R_{Fe}^2 + w^2 L_d L_q} (w L_d i_d - R_{Fe} i_q + w \psi_f) \quad (6)$$

$$i_{Fe \cdot q} = \frac{w L_d}{R_{Fe}^2 + w^2 L_d L_q} \left(w L_q i_q + R_{Fe} i_d + \frac{R_{Fe}}{L_d} \psi_f \right) \quad (7)$$

The copper and iron losses of PMSM can be deduced as follows [32]:

$$P_{cu} = R_s (i_d^2 + i_q^2) \quad (8)$$

$$P_{Fe} = R_{Fe} (i_{Fe.d}^2 + i_{Fe.q}^2) \quad (9)$$

The stray and mechanical losses are ignored in this study, therefore, the losses of PMSM can be simply calculated as:

$$P_{loss} = P_{Fe} + P_{cu} \quad (10)$$

Then, the efficiency of the PMSM can be calculated as:

$$\eta = \frac{P_{out}}{P_{out} + P_{loss}} \times 100\% = \frac{w T_e}{w T_e + P_{loss}} \quad (11)$$

From equations (6)-(10), it can be seen that the losses of PMSM depends on the speed, d-axis current, and q-axis current [29], as:

$$P_{loss} = f(w, i_d, i_q, i_{Fe.d}, i_{Fe.q}) \quad (12)$$

where P_{loss} is the total value of PMSM loss When the system is in a steady state, w and T_e are both constants, then the i_{sq} can be obtained by (2).

$$i_{sq} = \frac{T_e}{n_p(\psi_f + (L_d - L_q) i_{sd})} \quad (13)$$

To simplify the optimization process and reduce the control variables, we substitute (6), (7) and (13) into (8)-(9) to eliminate the variables of speed and q-axis current. Therefore, the iron loss and copper loss can be calculated just using the d-axis current, as follows:

$$P_{cu} = R_s \left\{ \left[i_{sd} - \frac{w L_q T_e}{P R_{Fe}(\psi_f + (L_d - L_q) i_{sd})} \right]^2 + \left[\frac{T_e}{P(\psi_f + (L_d - L_q) i_{sd})} + \frac{w(\psi_f + L_d i_{sd})}{R_{Fe}} \right]^2 \right\} \quad (14)$$

$$\begin{aligned} P_{Fe} &= R_{Fe}(i_{Fe.d}^2 + i_{Fe.q}^2) \\ &= \frac{\omega^2}{R_{Fe}^2} \left\{ (\psi_f + L_d i_{sd})^2 + \left[\frac{T_e L_q}{P(\psi_f + (L_d - L_q) i_{sd})} \right]^2 \right\} \quad (15) \end{aligned}$$

The iron loss of the PMSM can also be calculated by the eddy current and hysteresis as [30]:

$$P_{Fe} = K_e(1+s^2)a^2\psi_f^2 + k_h(1+s)a\psi_f^2 \qquad (16)$$

$$a = \frac{w_e}{w_b} = \frac{w_s + w_r}{w_b} \qquad (17)$$

$$s = \frac{w_s}{w_e} = \frac{w_s}{w_s + w_r} \qquad (18)$$

where K_e is the eddy current and its value is 0.0338, K_h is the hysteresis coefficients and its value is 0.0338, w_s is the slip speed, w_e is the supply frequency, w_r is the rotor speed, w_b is the base speed.

From (4), (9) and (16), the iron loss equivalent resistance of the PMSM can be deduced as:

$$R_{Fe} = \frac{w^2[L_d^2 i_{sq}^2 + (L_d i_{sd} + \psi_f)^2]}{K_e(1+s^2)a^2\psi_f^2 + k_h(1+s)a\psi_f^2} \qquad (19)$$

B. LOSS ANALYSIS

Fig. 2 gives motor loss under different speed and d-axis current, it shows that the motor loss equation is a convex function related to the d-axis current and speed of the PMSM.
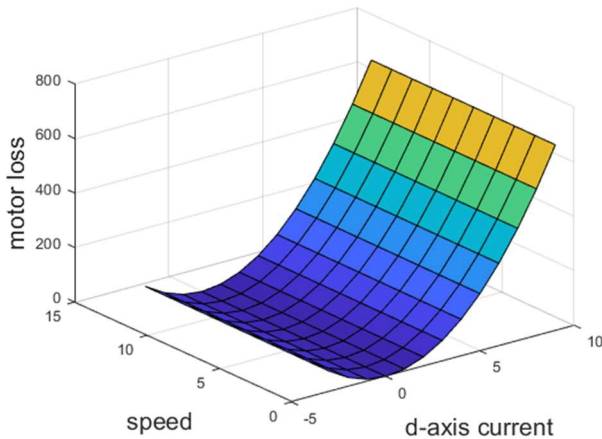

FIGURE 2. Motor loss under different speed and d-axis current.

When the PMSM is running under steady-state conditions. On the one hand, as the stator current excitation component decreases, according to (1), the magnetic flux value will reduce that results in the reduction in iron loss [31]. On the other hand, since the electromagnetic torque is proportionate to the magnetic flux and the torque current, to maintain the electromagnetic torque constant, the torque current will increase accordingly, thereby raising the copper loss. There is a balance point in the process of rising and falling, at this point, the iron loss and the copper loss reach a balance, and their sum is the smallest. Therefore, for any given speed-torque operating condition, there is a minimum total loss, and thereby the PMSM efficiency is the highest.

Ⅲ. EFFICIENCY OF PROPOSED OPTIMIZATION METHOD

A.AR-DPSO

Traditional PSO is difficult to track the optimal value under non-stationary operating conditions due to premature aggregation of particles. To solve this problem, the DPSO [25] and the ARPSO [26] are fused into the traditional PSO to guarantee that the particles have a certain self-regulation ability under non-stationary operating conditions, thereby ensuring that the proposed algorithm has a better adaptation to variation of external operating conditions. This algorithm is different from the velocity and position update equations in the traditional PSO. In the proposed AR-DPSO, the equations (20) and (21) are used to determine the velocity and position of the particle at the next moment in the iteration process, as bellow:

$$v_j(i+1) = \kappa \left[\begin{array}{c} v_j(i) + \frac{\phi}{2}c_p\sigma(x_j^{pbest} - x_j(i)) \\ + \frac{\phi}{2}c_g\sigma(x_j^{gbest} - x_j(i)) \end{array} \right] \qquad (20)$$

$$x_j(i+1) = x_j(i) + v_j(i+1) \qquad (21)$$

where i is the number of iterations of the PSO, j denotes the specific particle selected in each small cycle, $v_j(i)$ and $x_j(i)$ are the speed and position of the j particle in the i iteration respectively, and x_j^{pbest} and x_j^{gbest} are the individual optimal value and the overall optimal value of the j particle in the whole iterative process respectively, c_p and c_g denote random numbers between 0 and 1, κ represents the compression factor, (22) is its calculation formula, ϕ is a fixed constant, σ is used to judge whether diversity is needed, particle swarm shrinks when $\sigma = 1$, and particle swarm repels when $\sigma = -1$.

$$\kappa = \frac{2}{|2 - \phi - \sqrt{\phi^2 - 4\phi}|} \qquad (22)$$

The fitness value of each particle always changes in the non-stationary operating conditions that may lead to the d-axis current falling into a suboptimal solution. In this study, an evaporation mechanism is fused into the PSO to limit the change of the optimal value of the whole swarm, which can ensure that after the evaluation of every particle, the personal and global best solutions can update. The evaporation constant can be calculated as follows:

$$F_j(i+1) = \begin{cases} F_j(i) \times T & \text{if } f(X_j(i+1)) \le f(F_j(i)) \times T \\ x_j(i+1) & \text{if } f(X_j(i+1)) > f(F_j(i)) \times T \end{cases} \qquad (23)$$

$$T = \begin{cases} T_1 & \text{if } J \ge (1+k)J_{best}(j) \text{ or } J \le (1-k)J_{best}(j) \\ T_2 & \text{if } (1-k)J_{best}(j) < J < (1+k)J_{best}(j) \end{cases} \qquad (24)$$

where F represents the optimal value of the particle swarm in the iterative process, J denotes the fitness value of the j-th particle in the i-th iteration, T is the evaporation constant, and $J_{best}(j)$ represents the value of optimal PMSM losses obtained by the particles during each iteration, and it is also used to judge the size of T, $f(F)$ is particle's previous personal best fitness value, $f(X)$ denotes the current fitness value that the particle acquired.
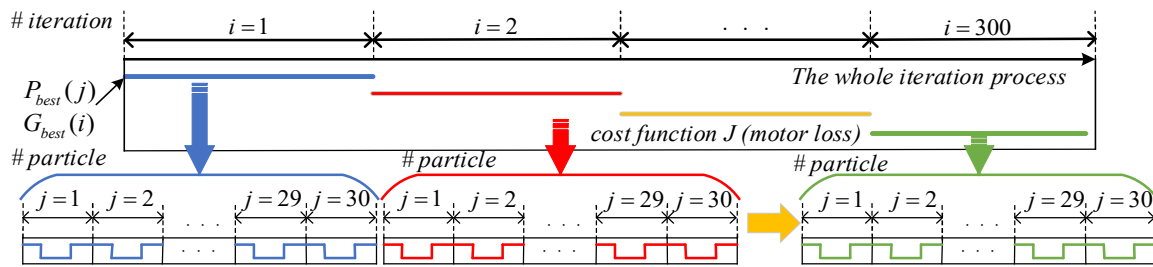
FIGURE 3. Structure of online AR-DPSO.

In the non-stationary operating conditions, another major problem of the traditional PSO is the premature convergence, which can cause part of the iteration to be meaningless. To make the particles have the ability to detect and respond to the dynamic and noisy environment, the diversity mechanism is added to the PSO to guarantee that when the environment changes greatly, the algorithm will select the appropriate diversity constant to shrink or gather the particle swarm, thereby avoiding premature aggregation. This mechanism can be described using equations (25) and (26), as below:

$$\sigma = \begin{cases} 1 & \text{if } \sigma < 0 \wedge D_{dir} > D_{threold} \\ -1 & \text{if } \sigma > 0 \wedge D_{dir} < D_{threold} \end{cases} \quad (25)$$

$$D_{dir} = \frac{x_{max}(i) - x_{min}(i)}{2} \quad (26)$$

where σ is the diversity constant, D_{dir} denotes the diversity threshold, $x_{max}(i)$ and $x_{max}(j)$ represent the maximum and minimum d-axis current values found in each iteration respectively, and $D_{threold}$ denotes a threshold that controls the range of particle swarm diversity [33].

The fitness function of AR-DPSO can be described as follows:

$$J = P_{loss} = P_{Cu} + P_{Fe} \quad (22)$$

In the algorithm, the positions of the particles are equivalent to the value of the d-axis current in the control circuit. The structure of the proposed online AR-DPSO is shown in Fig. 3.

B. AR-DPSO STEPS

The detailed steps of the AR-DPSO for PMSM are as follows:

(1) Initialize the position and velocity of particle, then use the optimal current obtained by the loss controller of the improved GSM-SC as the initial search value for AR-DPSO algorithm, and finally calculate the corresponding PMSM loss;

(2) Judge whether the number of iterations and the total number of particles have reached their maximum values;

(3) Randomly generate particles near the initial value of the algorithm, calculate the fitness value of each particle according to their initial position and velocity, calculate the individual optimal value *Pbest* and the group optimal value *Gbest*;

(4) Judge whether $Pbest(i)*T \le J$, if yes, then $Pbest(i) = Pbest(i)*T$, otherwise proceed to step (6);

(5) Judge whether $Gbest*T \le Pbest(i)$, if yes, judge whether $j \le 30$, and ensure that each particle participates in the process of optimization, otherwise proceed to step (7);

(6) Update the individual optimal value *Pbest*, update the speed and position of particle, and return to step (2);

(7) Update the group optimal value *Gbest*, update the speed and position of particle, and return to step (2);

(8) Calculate the diversity of the particle swarm, use the diversity mechanism to avoid particle aggregation, and update the particle properties, then return to step (2).

C. IMPROVED GSM-SC CONTROL STRATEGY

In the traditional PSO, the initialization process is random. Although this can guarantee the uniform distribution of the initial solution, but it cannot guarantee the quality of the individual, so that part of the particles are far away from the optimal solution. Similarly, due to the randomness of particle initialization, *Pbest* and *Gbest* are blinder. If choosing a better initial solution, it can not only reduce calculation time, but also improve the quality of the solution.

The initial solution of the AR-DPSO in this paper is obtained by the GSM-SC, but the traditional GSM-SC initially needs to use trial and error in the range of $(-\infty, 0)$ to find the optimal solution interval. This process will consume a lot of time, the success-failure method can start from a certain initial point and continuously search with the initial step length to find the GSM-SC search space. This algorithm steps are shown in Fig. 4, where ε denotes the accuracy value of the algorithm, h_0 represent the initial step size, I_{d1}, I_{d2}, I_{d3} and I_{d4} represent the stator current values in different iterations, P_{loss1}, P_{loss2} and P_{loss3} represent the PMSM loss under different current, I_{d5} is the optimal d-axis current.

D. EFFICIENCY OPTIMIZATION STRATEGY FOR PMSM

In this paper, the loss controller for PMSM is proposed based on GSM-SC and AR-DPSO. The block diagram of the optimization process is shown in Fig.5. The controller in Fig.5 receives the load torque, rotor speed and fitness function (efficiency equation), and then it determines the d-axis current value at which the maximum efficiency occurs at that rotor speed and load torque. The following research content will discuss the performance of this controller.

IV. COMPARATIVE EXPERIMENTAL RESULTS

A. SIMULATION RESULTS BASED ON GSM-SC

To verify the effectiveness of proposed control strategy for PMSM, Simulink was used to construct the PMSM efficiency optimization control circuit based on vector control in this

paper. The d-axis current in the control circuit is a variable, its value is obtained by the loss controller based on the success-failure method and GSM-SC. The parameters of PMSM are shown in Table 1.
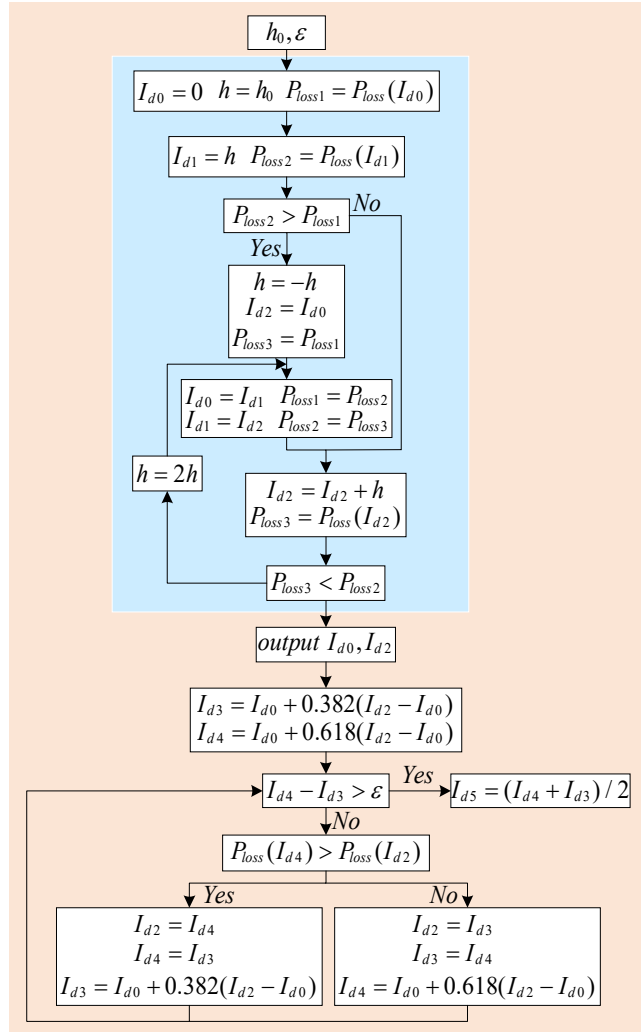

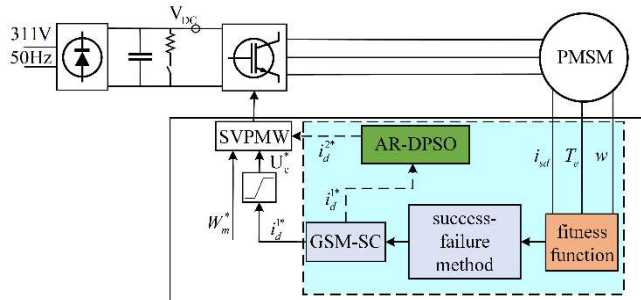**FIGURE 4. Flowchart of success-failure method and GSM-SC.**

FIGURE 5. Block diagram of PMSM drive system.

The PMSM is running under variable-speed-constant-torque and variable-torque-constant-speed conditions. The simulation duration is set to 0.7s. Fig. 6(a) is the response diagram of the PMSM under variable-torque-constant-speed

conditions. At the beginning, the PMSM runs at an initial torque of 7$N\cdot m$, and the speed is set to 60rad/min. After 0.3s, the PMSM torque becomes 14$N\cdot m$. After 0.5s, the PMSM operating conditions will change again, the loss controller will detect the change of the environment and alter the d-axis current. Fig. 6 (b) shows the operation process of the PMSM under variable-speed-constant-torque conditions. Throughout the whole process, PMSM needs to repeat the following operating conditions: reach the reference speed within the set time, when the operation is stable, the speed needs to be reduced to 0rad/min. The reference speeds are 30rad/min, 60rad/min, and 100rad/min respectively. Under these two non-stationary conditions, the optimal d-axis current obtained by the loss controller offline search can satisfy the high efficiency operation of the PMSM, which proves the robustness of the loss controller based on the GSM-SC.

TABLE 1. Parameters of PMSM

Descriptions	System Parameters	Values
J	equivalent rotor inertia	5.066×10^{-3}Kg/m^2
L_s	stator inductances	15.57×10^{-3}H
R_s	stator phase resistance	0.83ohm
ψ_f	flux linkage	0.2667Wb
B	viscous friction coefficient	0.0074$N\cdot m\cdot s$
R_{Fe}	iron loss equivalent resistance	49ohm
T_L	rated torque	14N/m

B. SIMULATION RESULTS BASED ON AR-DPSO

When PMSM is operating under constant-torque-variable-speed conditions and constant-speed-variable-torque conditions, the operating processes of the loss controller built by AR-DPSO can be described as follows:

1) The optimal d-axis current obtained by the GSM-SC is used as the initial searching value for the AR-DPSO to start the PMSM in the control circuit.

2) At the 100th and 200th iteration, the PMSM speed or torque will change.

4) Each iteration uses 30 particles. When the maximum number of iterations is 300, the iteration is terminated.

In the minimum loss control algorithm, the loss controller based on the AR-DPSO provides the stator d-axis current online and uses it in the control circuit, finally compares the operating efficiency of the PMSM under different conditions. To determine whether the proposed AR-DPSO will increase the computational burden, the simulation time of the proposed algorithm with ARPSO and DPSO is compared under the same operating conditions. Table 2 shows their calculation time, and it can be seen that the proposed AR-DPSO will slightly increase the computational burden, but the impact is not significant as compared with ARPSO and DPSO.

TABLE 2. Comparison of simulation time

Algorithm	Simulation time(s)
ARPSO	7457.70
DPSO	7690.50
AR-DPSO	8167.57
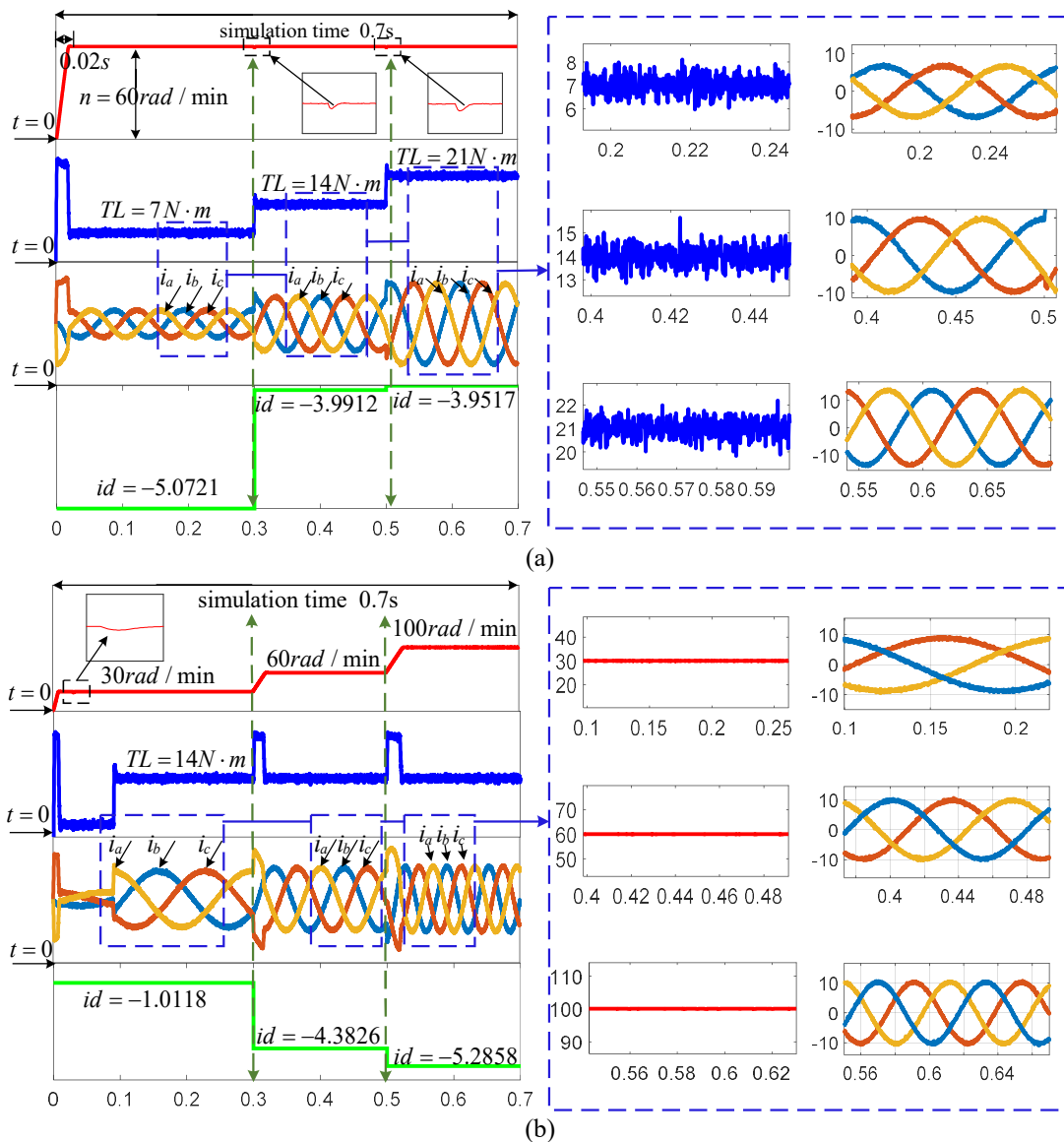
FIGURE 6. Motor response diagram based on GSM-SC. (a) Constant-speed (60*rad/min*)-variable torque (7 *N·m* -14 *N·m* -21*N·m*) conditions. (b) Constant-torque (14*N·m*)-variable speed (30 *rad/min* -60*rad/min* -100*rad/min*) conditions.

Fig. 7 shows the particle trajectory and PMSM losses with AR-DPSO, where the particle position represents the value of the d-axis current. It can be seen from Fig. 7 that the total PMSM loss and stator d-axis current will change with iteration, and eventually reach a stable value. This indicates that the AR-DPSO based on loss controller can control the d-axis current by improving the PMSM dynamic performance, thereby reducing loss. In Fig. 7, although the overall trend of particle swarm movement is gradually converging, some particles also deviate from the optimal position during the iteration processes. This is due to the existence of the diversity mechanism, the diversity threshold is larger. Fig. 8 shows the local velocity response of PMSM during particle swarm iteration processes. It can be seen from Fig. 8 (a) that under the constant speed conditions (60*rad/min*), the PMSM can quickly recover to the reference speed when the load torque (7*N·m*-14*N·m*-21*N·m*) is applied.

When the PMSM is running under constant-torque (14*N·m*)-variable-speed (30*rad/min*-60*rad/min*-100*rad/min*) conditions, it can be seen from Fig. 8 (b) that when the speed of PMSM rises to the reference speed, although the speed is a bit overshoot at the beginning, but it still has a faster dynamic response speed. Therefore, the PMSM control circuit based on the loss controller has a better dynamic performance and anti-disturbance ability. In the real-time control of the loss controller with AR-DPSO, each particle participates in the optimization process. The global optimal value will be adjusted in real time according to the PMSM loss obtained by the feedback of the control circuit in the iteration process, and the particle position corresponding to the optimal value will be used as the initial position of the particle swarm in the next iteration, the iteration will be repeated until the global optimal value is found.
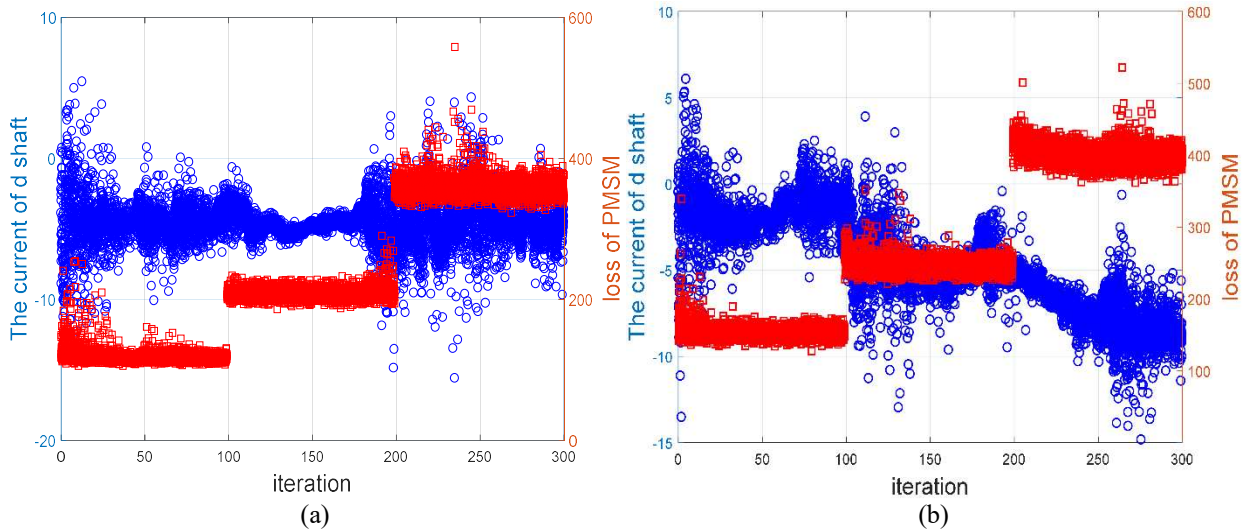
FIGURE 7. Optimal d-axis current and PMSM loss graph. (a) Constant-speed (60*rad/min*)-variable-torque (7*N·m*-14 *N·m*-21*N·m*) conditions. (b) Constant-torque-(14N·m)-variable-speed (30*rad/min*-60*rad/min*-100*rad/min*) conditions.
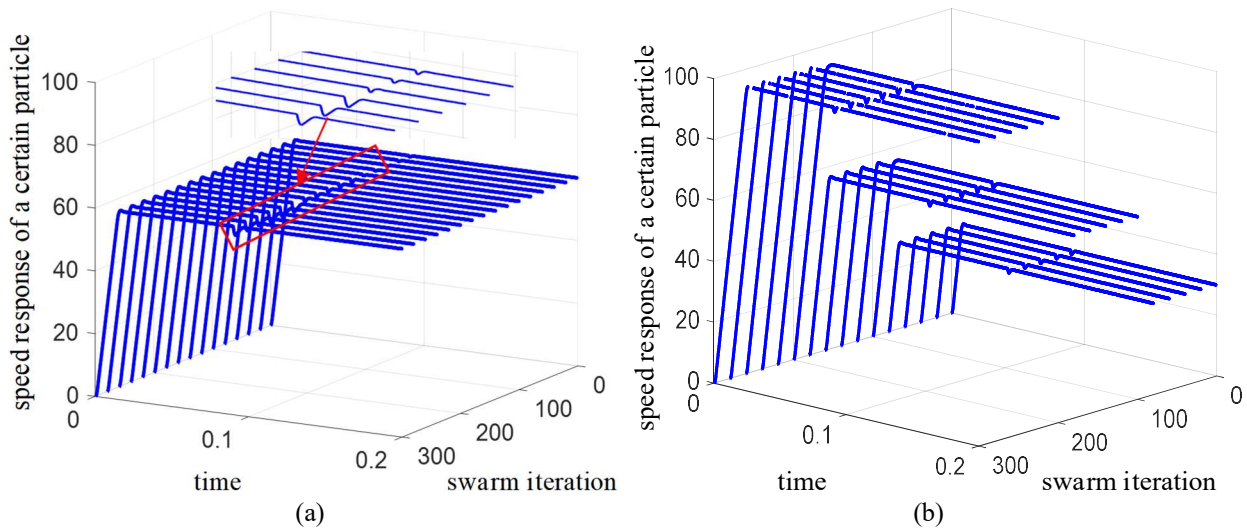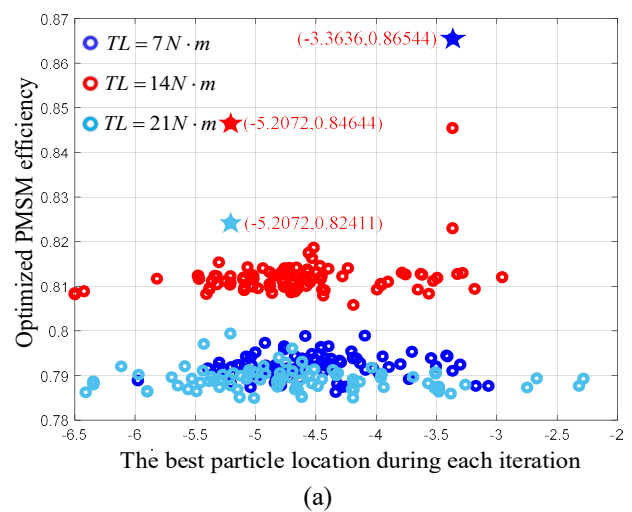

FIGURE 8. Motor speed response graph. (a) Constant-speed (60*rad/min*)-variable-torque (7*Nm*-14*Nm*-21*Nm*) conditions. (b) Constant-torque (14N·m)-variable-speed (30*rad/min*-60*rad/min*-100*rad/min*) conditions.

In the whole iteration process, different iteration processes correspond to the different PMSM speeds. The fitness function optimized by the AR-DPSO is the loss function of the PMSM. Initial particle position of the AR-DPSO is given by the loss controller built by the improved GSM-SC control strategy. The purpose of the optimization problem is to determine the ideal value of the d-axis current. To facilitate data statistics, the best and worst particles in each local iteration process will be recorded as shown in Fig. 9. The best particle position and its corresponding operating efficiency in every 100 iterations are highlighted in the picture. In the whole iteration process, the worst particles can still have a relatively stable output efficiency for PMSM as shown in Fig. 9 (b) and (d), which indicates that the algorithm has a great robustness. To sum up, comparing the simulation results with the GSM-SC algorithm, the AR-DPSO algorithm can not only guarantee good steady-state performance in non-stationary operation conditions, but also search the best d-axis current value more accurately.

(a)

(b)

(c)

(d)
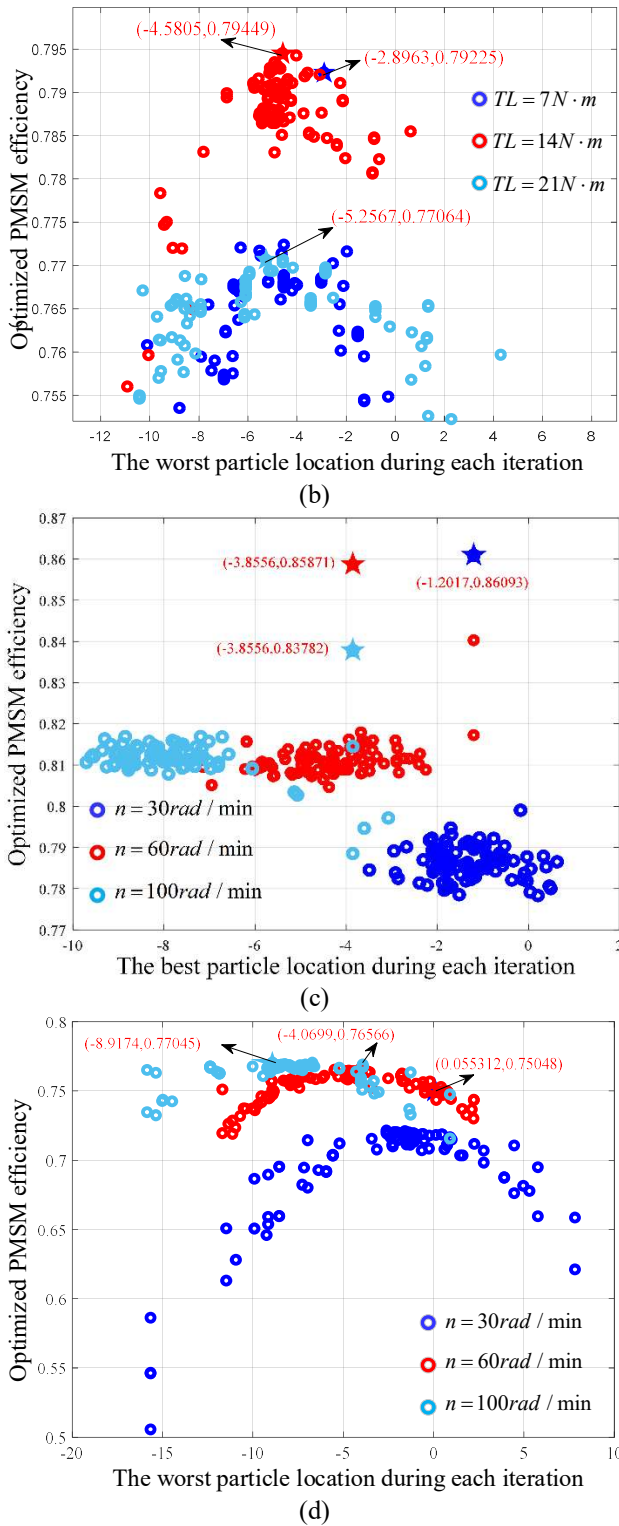
FIGURE 9. Particle trajectory. (a) The best particle set in each iteration under constant-speed (60*rad/min*) –variable-torque (7*N·m*-14*N·m*-21*N·m*) conditions. (b) The worst particle set in each iteration under constant-speed (60*rad/min*)-variable-torque (7*N·m*-14*N·m*-21*N·m*) conditions. (c) The best particle set in each iteration under constant-torque (14*N·m*)-variable-speed (30*rad/min*-60*rad/min*-100*rad/min*) conditions. (d) The worst particle set in each iteration under constant-torque (14*N·m*)-variable-speed (30*rad/min*-60*rad/min*-100*rad/min*) conditions.

To facilitate data statistics, the best and worst particles in each local iteration process are recorded as shown in Fig. 9.

The best particle position and its corresponding operating efficiency in every 100 iterations are highlighted in the picture. It can be seen that, in the whole iteration process, the worst particles can still have a relatively stable output efficiency for PMSM as shown in Fig. 9 (b) and (d). This indicates that the algorithm has a great robustness. As compared the simulation results with the GSM-SC algorithm, the AR-DPSO can not only guarantee good steady-state performance in non-stationary operating conditions, but also search the best d-axis current more accurately.

*C. COMPARATIVE EXPERIMENTAL RESULTS*

Table 3 and Table 4 summarize the optimized d-axis current, copper losses and iron losses of the three control algorithms based on different d-axis current under non-stationary working conditions.

TABLE 3. Comparison of PMSM loss of the three control modes under constant-speed (60*rad/min*)-variable-torque (7*N·m*-14*N·m*-21*N·m*) conditions.

Control Method	$T_L(N \cdot m)$	id(A)	$P_{Cu}(W)$	$P_{Fe}(W)$	$P_{Loss}(W)$
id=0	7	0	31.66	116.3	147.96
	14	0	99.11	130.08	229.19
	21	0	216.7	173.35	392.05
GSM-SC	7	-5.07	56.17	61.05	141.29
	14	-3.99	131.0	95.28	226.28
	21	-3.95	236.7	133.9	370.6
AR-DPSO	7	-3.36	43.25	62.51	105.76
	14	-5.21	87.51	66.14	153.65
	21	-5.21	198.63	70.29	268.92

TABLE 4. Comparison of PMSM loss of the three control modes under constant-torque (14*N·m*)-variable-speed (30*rad/min*-60*rad/min*-100*rad/min*) conditions.

Control Method	$Nr(rad/min)$	id(A)	$P_{Cu}(W)$	$P_{Fe}(W)$	$P_{Loss}(W)$
id=0	30	0	100.6	32.81	133.41
	60	0	98.73	136.11	234.84
	100	0	115.4	384.48	499.88
GSM-SC	30	-0.39	89.13	31.44	120.57
	60	-4.39	114	88.14	202.14
	100	-6.39	136.5	221.47	357.97
AR-DPSO	30	-0.69	84.29	21.35	105.64
	60	-5.15	95.25	64.39	159.64
	100	-5.15	112.6	158.4	271.00

Fig. 10 (a) shows the losses of motor as using three different control algorithms under constant-speed-variable-torque conditions, it can be seen from Fig. 10(a) that under the low-torque condition (7*N·m*), the iron loss accounts for a large proportion of the total losses. With the optimization of the AR-DPSO, the efficiency of the PMSM changes from 73.77% to 86.544%, and it is improved by 12.774%, although the AR-DPSO will reduce the overall loss, the copper loss is increased. This is because the current consumed by the equivalent iron resistance of the PMSM is inversely proportional to the current consumed by the stator winding resistance. When the algorithm focuses on reducing the iron loss, that is, reducing the current consumed by the equivalent iron resistance, the current consumed by the stator winding resistance is increased. Therefore, the algorithm needs to be further optimized to ensure that the overall PMSM loss can be optimized under low load torque conditions, and the copper loss and iron loss can

be optimized separately. When the torque reaches 14$N\cdot m$, the PMSM copper loss increases relatively. Compared with GSM-SC, the AR-DPSO has a better optimization effect on copper loss, the copper loss reduces from 131W to 87.51W, and the overall losses are reduced by 72.63W. When the torque reaches 21$N\cdot m$, the losses are increased relatively compared with the low torque condition. In the traditional id=0 control, the total losses reached 392.05W. Obviously, for this PMSM, id=0 is not the optimal current value. The loss controller built by the GSM-SC can reduce the losses to 370.6W, however, compared with the traditional id=0 control, the copper loss at this time has increased. The loss controller built based on AR-DPSO reduces the iron loss to 70.29W and reduces the copper loss to 198.23W. Compared with the previous two control algorithms, the overall operating efficiency of the PMSM has been greatly improved.
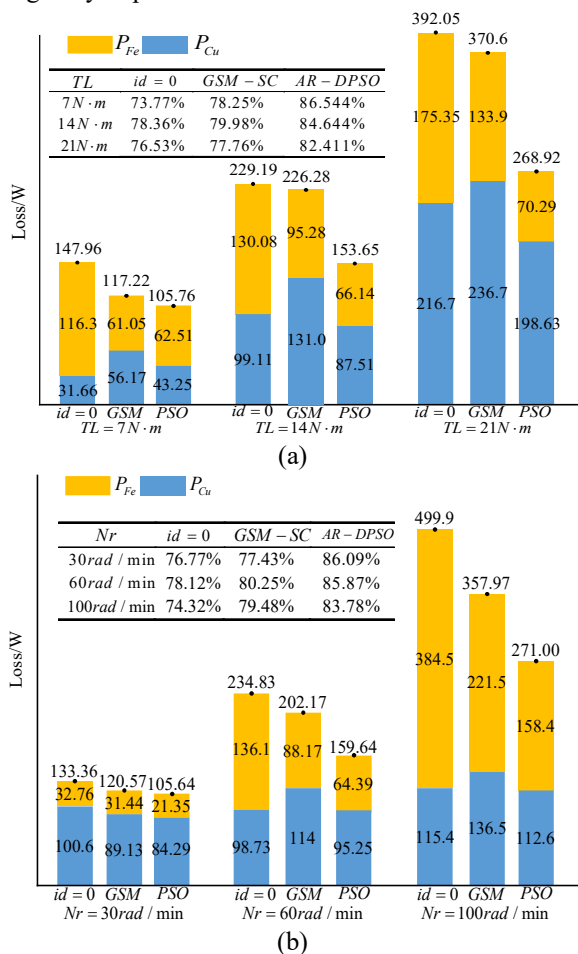
At this time, the PMSM output power is also low. With the loss controller built based on AR-DPSO working, the efficiency changes from 76.77% to 86.05 with 9.28% improvement. When the speed reaches 60rad/min, the iron loss increases relatively. The loss controller built based on AR-DPSO has a better optimization effect on iron loss. The iron loss is reduced from 136.1W to 64.39W. When the speed reaches 100rad/min, in the traditional id=0 control, the iron loss is not optimized, and the iron loss is 384.5W. The loss controller built by GSM-SC can reduce the iron loss to 221.5W. The loss controller built based on the improved PSO reduces the iron loss to 158.4W, the total losses are reduced by 228.9W compared with the traditional id=0 control. It is analyzed that the loss controller built based on the AR-DPSO will be better than the loss controller based on the GSM-SC under constant-torque-variable-speed and constant-speed-variable-torque conditions.

V. CONCLUSION

In this paper, an improved particle swarm optimization (AR-DPSO) is proposed to improve the operating efficiency of PMSM through combining the attraction and repulsion particle swarm optimization and the distributed particle swarm optimization. The proposed algorithm can find the optimal d-axis air gap current online in a non-stationary state that can minimize the air gap flux, and then improve the overall operating efficiency of PMSM. This algorithm can avoid the d-axis air gap current falling into a local optimal value as that encountered using the traditional particle swarm optimization. To verify the effectiveness and stability of this proposed algorithm, we compared the algorithm with the traditional golden section method under the constant-speed-variable-torque and constant-torque-variable-speed conditions. The simulation results reveal that the proposed algorithm can improve the operating efficiency of PMSM by 5.870% on average under the constant-speed-variable-torque conditions, and by 6.193% on average under the constant-torque-variable-speed conditions. This indicates that the proposed AR-DPSO has a better adaptation to variation of external operating conditions, and can actually improve the operation efficiency of the PMSM under non-stationary operating conditions. The results also show that the proposed algorithm has a promising application in the efficiency optimization control of PMSM, and can provide a significant reference for optimizing traditional search algorithms.

Considering that when the PMSM is operating under low load torque conditions, although the AR-DPSO will reduce the overall loss, the copper loss is increased. Therefore, in the future, the algorithm needs to be further optimized to ensure that the whole loss can be optimized under low load torque conditions, and the copper loss and iron loss can be optimized separately. At the same time, more in-depth analysis in terms of the relationship between the real-time optimal current, speed and torque will be conducted.

FIGURE 10. Comparison chart of motor efficiency under three control algorithms. (a) Constant-speed (60rad/min)-variable-torque (7$N\cdot m$ -14$N\cdot m$ -21$N\cdot m$) conditions. (b) Constant-torque (14$N\cdot m$)-variable speed (30rad/min-60rad/min-100rad/min) conditions.

Fig. 10 (b) shows the losses values based on three different control algorithms under constant-torque-variable-speed conditions, it can be seen from Fig. 10 (b) that the copper loss and iron loss of the PMSM increase with the change of speed, where the increase in iron loss is more obvious as the speed increases. Under the low speed condition (30rad/min), the copper loss accounts for a large proportion of the total losses.

REFERENCES

[1] Zhang C, Yang F, Ke XY, Liu ZF and Yuan C, "Predictive modeling of energy consumption and greenhouse gas emissions from autonomous electric vehicle operations," *Appl. Energy*, vol. 254, no. 10, 2019.

[2] Y. Liu, J. Li, Z. Chen, D. Qin, Y. Zhang, "Research on a multi-objective hierarchical prediction energy management strategy for range extended fuel cell vehicles," *J. Power Sources*, vol. 429, pp. 55–66, 2019.

[3] Shu X, Li G, Shen JW, Yan WS, Chen Z and Liu YG, "An adaptive fusion estimation algorithm for state of charge of lithium-ion batteries considering wide operating temperature and degradation," *J Power Sources*, vol. 462, pp. 13, 2020.

[4] Xiaofeng Ding, Min Du, Chongwei Duan, Hong Guo, Rui Xiong, Jinquan Xu, Jiawei Chen, Partrick Chi kwong Luk, "Analytical and experimental evaluation of SiC-inverter nonlinearities for traction drives used in electric vehicles," *IEEE Transactions on Vehicular Technology*, vol. 67, no. 1, pp: 146-159, Jan, 2018.

[5] Z. Shan, X. Ding, J. Jatskevich and C. K. Tse, "Synthesis of multi-input multi-output DC/DC converters without energy buffer stages," *IEEE Transactions on Circuits and Systems II: Express Briefs*, pp: 1558-3791, Aug, 2020.

[6] Chen Z, Hu HJ, Wu YT, Xiao RX, Shen JW and Liu YG, "Energy management for a power-split plug-in hybrid electric vehicle based on reinforcement learning," *Appl Sci-Basel*, vol. 8, pp. 15, 2018.

[7] J. Kim, S. Ryu, M. S. Rafaq, H. H. Choi and J. Jung, "Improved torque ripple minimization technique with enhanced efficiency for surface-mounted PMSM drives," *IEEE Access*, vol. 8, pp. 115017-115027, 2020.

[8] Teng F, Mu YF, Jia HJ, Wu JZ, Zeng PL and Strbac, "Challenges on primary frequency control and potential solution from EVs in the future GB electricity system," *Appl Energy*, vol. 194, pp. 353-362, 2017.

[9] Guo QB, Zhang CM, Li LY, Gerada D, Zhang JP and Wang M, "Design and implementation of a loss optimization control for electric vehicle in-wheel permanent-magnet synchronous motor direct drive system," *Appl Energy*, vol. 204, pp. 1317-1332, 2017.

[10] Li K and Wang Y, "Maximum torque per ampere (MTPA) control for IPMSM drives based on a variable-equivalent-parameter MTPA control law," *IEEE Trans Power Electron*, vol. 34, pp. 7092-7102, 2019.

[11] Ekanayake S, Dutta R, Rahman MF and Xiao D, "Direct torque and flux control of interior permanent magnet synchronous machine in deep flux-weakening region," *IET Electr Power Appl*, vol. 12, pp. 98-105, 2018.

[12] Riadh Abdelati,M and Faouzi Mimouni, "Optimal control strategy of an induction motor for loss minimization using Pontryaguin principle," *European Journal of Control*, 2019, 49: 94-106.

[13] Jeyashanthi J and Santhi M, "Improved efficiency of direct torque controlled induction motor drive by golden section method," *Revista Facultad de Ingeniería Universidad de Antioquia*, vol. 91, pp. 31-41, 2019.

[14] Yousefi-Talouki A, Pescetto P, Pellegrino G and Boldea I, "Combined active flux and high-frequency injection methods for sensorless direct-flux vector control of synchronous reluctance machines," *IEEE Trans Power Electron*, vol. 33, pp. 2447-2457, 2018.

[15] W. Jiang, S. Feng, Z. Zhang, J. Zhang and Z. Zhang, "Study of efficiency characteristics of interior permanent magnet synchronous motors," *IEEE Transactions on Magnetics,* vol. 54, no. 11, pp. 1-5, 2018.

[16] Liu Q and Hameyer K, "High-performance adaptive torque control for an IPMSM with real-time MTPA operation," *IEEE Trans Energy Convers*, vol. 32, pp. 571-581, 2017.

[17] Zhang DD, Liu TH, Zhao HS and Wu T, "An analytical iron loss calculation model of inverter-fed induction motors considering supply and slot harmonics," *IEEE Trans Ind Electron*, vol. 66, pp. 9194-9204, 2019.

[18] Kioskeridis I and Mademlis C, "Energy efficiency optimisation in synchronous reluctance motor drives," *IEE Proc-Electr Power Appl*, vol. 150, pp. 201-209, 2003.

[19] Jeyashanthi J and Santhi M, "Improved efficiency of direct torque controlled induction motor drive by golden section method," *Revista Facultad de Ingeniería Universidad de Antioquia*, pp. 31-42, 2019.

[20] Mutluer M, Sahman MA and Cunkas M, "Heuristic optimization based on penalty approach for surface permanent magnet synchronous," *Arab J Sci Eng*, vol 17, 2020.

[21] Ni RG, Xu DG, Wang GL, Ding L, Zhang GQ and Qu LZ, "Maximum efficiency per ampere control of permanent-magnet synchronous machines," *IEEE Trans Ind Electron*, vol. 62, pp. 2135-2143, 2015.

[22] Hesari S and Hoseini A, "A new approach to improve induction motor performance in light-load conditions," *J Electr Eng Technol*, vol. 12, pp. 1195-1202, 2017.

[23] Kim DH and Hirota K, "Vector control for loss minimization of induction motor using GA-PSO," *Appl Soft Comput.* vol. 8, pp. 1692-1702, 2008.

[24] W. Liu, I. Chung, S. Leng and D. A. Cartes, "Real-time particle swarm optimization based current harmonic cancellation," in 2009 IEEE Power & Energy Society General Meeting, Calgary, AB, 2009, pp. 1-7.

[25] Jacques Riget, Jakob S. Vesterstrøm, "A diversity-guided particle swarm optimizer - the ARPSO," *Evalife Technical Report*, 2002.

[26] Cui XH, St Charles J and Potok TE, "A simple distributed particle swarm optimization for dynamic and noisy environments," in Nature Inspired Cooperative Strategies for Optimization (NICSO 2008), Rome, 2009, pp. 89-102.

[27] Szczepanski R, Tarczewski T and Grzesiak LM, "Adaptive state feedback speed controller for PMSM based on Artificial Bee Colony algorithm," *Appl Soft Comput*, vol. 83, pp. 12, 2019.

[28] Sriprang S, Nahid-Mobarakeh B, Takorabet N, Pierfederici S, Kumam P, Bizon N, Taghavi N, Vahedi A, Mungporn P and Thounthong P, "Design and control of permanent magnet assisted synchronous reluctance motor with copper loss minimization using MTPA," *J Electr Eng*, vol. 71, pp. 11-19, 2020.

[29] Zhang DD, Liu TH, Zhao HS and Wu T, "An analytical iron loss calculation model of inverter-fed induction motors considering supply and slot harmonics," *IEEE Trans Ind Electron.* vol. 66, pp. 9194-9204, 2019.

[30] R. H. A. Hamid, A. M. A. Amin, R. S. Ahmed and A. A. A. El-Gammal, "New technique for Maximum Efficiency and Minimum Operating Cost of induction motors based on Particle Swarm Optmization (PSO)," in 2006 Eleventh International Middle East Power Systems Conference, El-Minia, 2006, pp. 416-420.

[31] Yamashita Y and Okamoto Y. "Design Optimization of Synchronous Reluctance Motor for Reducing Iron Loss and Improving Torque Characteristics Using Topology Optimization Based on the Level-Set Method," *IEEE Trans Magn*, vol. 56, pp. 4, 2020.

[32] Hwang HY and Chen JS, "Optimized fuel economy control of power-split hybrid electric vehicle with particle swarm optimization," *Energies.* vol. 13, pp. 18, 2020.

[33] Ufnalski B and Grzesiak LM, "Plug-in direct particle swarm repetitive controller with a reduced dimensionality of a fitness landscape - a multi-swarm approach," *Bull Pol Acad Sci-Tech Sci.* vol. 63, pp. 857-866, 2015.